

Fermi National Accelerator Laboratory

FERMILAB-Conf-96/247-E

DØ

Hard Single Diffractive Jet Production at DØ

S. Abachi et al.
The DØ Collaboration
*Fermi National Accelerator Laboratory
P.O. Box 500, Batavia, Illinois 60510*

August 1996

Submitted to the *28th International Conference on High Energy Physics*, Warsaw, Poland, July 25 - 31, 1996.

Disclaimer

This report was prepared as an account of work sponsored by an agency of the United States Government. Neither the United States Government nor any agency thereof, nor any of their employees, makes any warranty, express or implied, or assumes any legal liability or responsibility for the accuracy, completeness or usefulness of any information, apparatus, product or process disclosed, or represents that its use would not infringe privately owned rights. Reference herein to any specific commercial product, process or service by trade name, trademark, manufacturer or otherwise, does not necessarily constitute or imply its endorsement, recommendation or favoring by the United States Government or any agency thereof. The views and opinions of authors expressed herein do not necessarily state or reflect those of the United States Government or any agency thereof.

Distribution

Approved for public release: further dissemination unlimited.

Hard Single Diffractive Jet Production at DØ

The DØ Collaboration¹
(July 1996)

Preliminary results from the DØ experiment on jet production with forward rapidity gaps in $p\bar{p}$ collisions are presented. A class of dijet events with a forward rapidity gap is observed at center-of-mass energies $\sqrt{s} = 1800$ GeV and 630 GeV. The number of events with rapidity gaps at both center-of-mass energies is significantly greater than the expectation from multiplicity fluctuations and is consistent with a hard single diffractive process. A small class of events with two forward gaps and central dijets is also observed at 1800 GeV. This topology is consistent with hard double pomeron exchange.

S. Abachi,¹⁴ B. Abbott,²⁸ M. Abolins,²⁵ B.S. Acharya,⁴³ I. Adam,¹² D.L. Adams,³⁷ M. Adams,¹⁷
 S. Ahn,¹⁴ H. Aihara,²² J. Alitti,⁴⁰ G. Álvarez,¹⁸ G.A. Alves,¹⁰ E. Amidi,²⁹ N. Amos,²⁴
 E.W. Anderson,¹⁹ S.H. Aronson,⁴ R. Astur,⁴² R.E. Avery,³¹ M.M. Baarmand,⁴² A. Baden,²³
 V. Balamurali,³² J. Balderston,¹⁶ B. Baldin,¹⁴ S. Banerjee,⁴³ J. Bantly,⁵ J.F. Bartlett,¹⁴
 K. Bazizi,³⁹ J. Bendich,²² S.B. Beri,³⁴ I. Bertram,³⁷ V.A. Bezzubov,³⁵ P.C. Bhat,¹⁴
 V. Bhatnagar,³⁴ M. Bhattacharjee,¹³ A. Bischoff,⁹ N. Biswas,³² G. Blazey,¹⁴ S. Blessing,¹⁵
 P. Bloom,⁷ A. Boehnlein,¹⁴ N.I. Bojko,³⁵ F. Borcharding,¹⁴ J. Borders,³⁹ C. Boswell,⁹
 A. Brandt,¹⁴ R. Brock,²⁵ A. Bross,¹⁴ D. Buchholz,³¹ V.S. Burtovoi,³⁵ J.M. Butler,³
 W. Carvalho,¹⁰ D. Casey,³⁹ H. Castilla-Valdez,¹¹ D. Chakraborty,⁴² S.-M. Chang,²⁹
 S.V. Chekulaev,³⁵ L.-P. Chen,²² W. Chen,⁴² S. Choi,⁴¹ S. Chopra,²⁴ B.C. Choudhary,⁹
 J.H. Christenson,¹⁴ M. Chung,¹⁷ D. Claes,⁴² A.R. Clark,²² W.G. Cobau,²³ J. Cochran,⁹
 W.E. Cooper,¹⁴ C. Cretsinger,³⁹ D. Cullen-Vidal,⁵ M.A.C. Cummings,¹⁶ D. Cutts,⁵ O.I. Dahl,²²
 K. De,⁴⁴ M. Demarteau,¹⁴ N. Denisenko,¹⁴ D. Denisov,¹⁴ S.P. Denisov,³⁵ H.T. Diehl,¹⁴
 M. Diesburg,¹⁴ G. Di Loreto,²⁵ R. Dixon,¹⁴ P. Draper,⁴⁴ J. Drinkard,⁸ Y. Ducros,⁴⁰
 S.R. Dugad,⁴³ D. Edmunds,²⁵ J. Ellison,⁹ V.D. Elvira,⁴² R. Engelmann,⁴² S. Eno,²³ G. Eppley,³⁷
 P. Ermolov,²⁶ O.V. Eroshin,³⁵ V.N. Evdokimov,³⁵ S. Fahey,²⁵ T. Fahland,⁵ M. Fatyga,⁴
 M.K. Fatyga,³⁹ J. Featherly,⁴ S. Feher,¹⁴ D. Fein,² T. Ferbel,³⁹ G. Finocchiaro,⁴² H.E. Fisk,¹⁴
 Y. Fisyak,⁷ E. Flattum,²⁵ G.E. Forden,² M. Fortner,³⁰ K.C. Frame,²⁵ P. Franzini,¹² S. Fuess,¹⁴
 E. Gallas,⁴⁴ A.N. Galyaev,³⁵ T.L. Geld,²⁵ R.J. Genik II,²⁵ K. Genser,¹⁴ C.E. Gerber,¹⁴
 B. Gibbard,⁴ V. Glebov,³⁹ S. Glenn,⁷ J.F. Glicenstein,⁴⁰ B. Gobbi,³¹ M. Goforth,¹⁵
 A. Goldschmidt,²² B. Gómez,¹ G. Gomez,²³ P.I. Goncharov,³⁵ J.L. González Solís,¹¹ H. Gordon,⁴
 L.T. Goss,⁴⁵ N. Graf,⁴ P.D. Grannis,⁴² D.R. Green,¹⁴ J. Green,³⁰ H. Greenlee,¹⁴ G. Griffin,⁸
 N. Grossman,¹⁴ P. Grudberg,²² S. Gr̄unendahl,³⁹ W.X. Gu,^{14,*} G. Guglielmo,³³ J.A. Guida,²
 J.M. Guida,⁵ W. Guryñ,⁴ S.N. Gurzhiev,³⁵ P. Gutierrez,³³ Y.E. Gutnikov,³⁵ N.J. Hadley,²³
 H. Haggerty,¹⁴ S. Hagopian,¹⁵ V. Hagopian,¹⁵ K.S. Hahn,³⁹ R.E. Hall,⁸ S. Hansen,¹⁴
 R. Hatcher,²⁵ J.M. Hauptman,¹⁹ D. Hedin,³⁰ A.P. Heinson,⁹ U. Heintz,¹⁴
 R. Hernández-Montoya,¹¹ T. Heuring,¹⁵ R. Hirosky,¹⁵ J.D. Hobbs,¹⁴ B. Hoeneisen,^{1,†}
 J.S. Hoftun,⁵ F. Hsieh,²⁴ Tao Hu,^{14,*} Ting Hu,⁴² Tong Hu,¹⁸ T. Huehn,⁹ S. Igarashi,¹⁴ A.S. Ito,¹⁴
 E. James,² J. Jaques,³² S.A. Jeger,²⁵ J.Z.-Y. Jiang,⁴² T. Joffe-Minor,³¹ H. Johari,²⁹ K. Johns,²
 M. Johnson,¹⁴ H. Johnstad,²⁹ A. Jonckheere,¹⁴ M. Jones,¹⁶ H. Jöstlein,¹⁴ S.Y. Jun,³¹

¹Submitted to the 28th International Conference on High Energy Physics, Warsaw, Poland, 25-31 July 1996.

C.K. Jung,⁴² S. Kahn,⁴ G. Kalbfleisch,³³ J.S. Kang,²⁰ R. Kehoe,³² M.L. Kelly,³² L. Kerth,²²
 C.L. Kim,²⁰ S.K. Kim,⁴¹ A. Klatchko,¹⁵ B. Klima,¹⁴ B.I. Klochkov,³⁵ C. Klopfenstein,⁷
 V.I. Klyukhin,³⁵ V.I. Kochetkov,³⁵ J.M. Kohli,³⁴ D. Koltick,³⁶ A.V. Kostritskiy,³⁵ J. Kotcher,⁴
 J. Kourlas,²⁸ A.V. Kozelov,³⁵ E.A. Kozlovski,³⁵ M.R. Krishnaswamy,⁴³ S. Krzywdzinski,¹⁴
 S. Kunori,²³ S. Lami,⁴² G. Landsberg,¹⁴ J-F. Lebrat,⁴⁰ A. Leflat,²⁶ H. Li,⁴² J. Li,⁴⁴ Y.K. Li,³¹
 Q.Z. Li-Demarteau,¹⁴ J.G.R. Lima,³⁸ D. Lincoln,²⁴ S.L. Linn,¹⁵ J. Linnemann,²⁵ R. Lipton,¹⁴
 Y.C. Liu,³¹ F. Lobkowicz,³⁹ S.C. Loken,²² S. Lökös,⁴² L. Lueking,¹⁴ A.L. Lyon,²³
 A.K.A. Maciel,¹⁰ R.J. Madaras,²² R. Madden,¹⁵ L. Magaña-Mendoza,¹¹ S. Mani,⁷ H.S. Mao,^{14,*}
 R. Markeloff,³⁰ L. Markosky,² T. Marshall,¹⁸ M.I. Martin,¹⁴ B. May,³¹ A.A. Mayorov,³⁵
 R. McCarthy,⁴² T. McKibben,¹⁷ J. McKinley,²⁵ T. McMahon,³³ H.L. Melanson,¹⁴
 J.R.T. de Mello Neto,³⁸ K.W. Merritt,¹⁴ H. Miettinen,³⁷ A. Mincer,²⁸ J.M. de Miranda,¹⁰
 C.S. Mishra,¹⁴ N. Mokhov,¹⁴ N.K. Mondal,⁴³ H.E. Montgomery,¹⁴ P. Mooney,¹ H. da Motta,¹⁰
 M. Mudan,²⁸ C. Murphy,¹⁷ F. Nang,⁵ M. Narain,¹⁴ V.S. Narasimham,⁴³ A. Narayanan,²
 H.A. Neal,²⁴ J.P. Negret,¹ E. Neis,²⁴ P. Nemethy,²⁸ D. Nešić,⁵ M. Nicola,¹⁰ D. Norman,⁴⁵
 L. Oesch,²⁴ V. Oguri,³⁸ E. Oltman,²² N. Oshima,¹⁴ D. Owen,²⁵ P. Padley,³⁷ M. Pang,¹⁹
 A. Para,¹⁴ C.H. Park,¹⁴ Y.M. Park,²¹ R. Partridge,⁵ N. Parua,⁴³ M. Paterno,³⁹ J. Perkins,⁴⁴
 A. Peryshkin,¹⁴ M. Peters,¹⁶ H. Piekarz,¹⁵ Y. Pischalnikov,³⁶ V.M. Podstavkov,³⁵ B.G. Pope,²⁵
 H.B. Prosper,¹⁵ S. Protopopescu,⁴ D. Pušeljčić,²² J. Qian,²⁴ P.Z. Quintas,¹⁴ R. Raja,¹⁴
 S. Rajagopalan,⁴² O. Ramirez,¹⁷ M.V.S. Rao,⁴³ P.A. Rapidis,¹⁴ L. Rasmussen,⁴² S. Reucroft,²⁹
 M. Rijssenbeek,⁴² T. Rockwell,²⁵ N.A. Roe,²² P. Rubinov,³¹ R. Ruchti,³² J. Rutherford,²
 A. Sánchez-Hernández,¹¹ A. Santoro,¹⁰ L. Sawyer,⁴⁴ R.D. Schamberger,⁴² H. Schellman,³¹
 J. Sculli,²⁸ E. Shabalina,²⁶ C. Shaffer,¹⁵ H.C. Shankar,⁴³ R.K. Shivpuri,¹³ M. Shupe,²
 J.B. Singh,³⁴ V. Sirotenko,³⁰ W. Smart,¹⁴ A. Smith,² R.P. Smith,¹⁴ R. Snihur,³¹ G.R. Snow,²⁷
 J. Snow,³³ S. Snyder,⁴ J. Solomon,¹⁷ P.M. Sood,³⁴ M. Sosebee,⁴⁴ M. Souza,¹⁰ A.L. Spadafora,²²
 R.W. Stephens,⁴⁴ M.L. Stevenson,²² D. Stewart,²⁴ D.A. Stoianova,³⁵ D. Stoker,⁸ K. Streets,²⁸
 M. Strovink,²² A. Sznajder,¹⁰ P. Tamburello,²³ J. Tarazi,⁸ M. Tartaglia,¹⁴ T.L. Taylor,³¹
 J. Thompson,²³ T.G. Trippe,²² P.M. Tuts,¹² N. Varelas,²⁵ E.W. Varnes,²² P.R.G. Virador,²²
 D. Vititoe,² A.A. Volkov,³⁵ A.P. Vorobiev,³⁵ H.D. Wahl,¹⁵ G. Wang,¹⁵ J. Warchol,³² G. Watts,⁵
 M. Wayne,³² H. Weerts,²⁵ A. White,⁴⁴ J.T. White,⁴⁵ J.A. Wightman,¹⁹ J. Wilcox,²⁹ S. Willis,³⁰
 S.J. Wimpenny,⁹ J.V.D. Wirjawan,⁴⁵ J. Womersley,¹⁴ E. Won,³⁹ D.R. Wood,²⁹ H. Xu,⁵
 R. Yamada,¹⁴ P. Yamin,⁴ C. Yanagisawa,⁴² J. Yang,²⁸ T. Yasuda,²⁹ P. Yepes,³⁷ C. Yoshikawa,¹⁶
 S. Youssef,¹⁵ J. Yu,¹⁴ Y. Yu,⁴¹ Q. Zhu,²⁸ Z.H. Zhu,³⁹ D. Zieminska,¹⁸ A. Zieminski,¹⁸
 E.G. Zverev,²⁶ and A. Zylberstein⁴⁰

¹Universidad de los Andes, Bogotá, Colombia

²University of Arizona, Tucson, Arizona 85721

³Boston University, Boston, Massachusetts 02215

⁴Brookhaven National Laboratory, Upton, New York 11973

⁵Brown University, Providence, Rhode Island 02912

⁶Universidad de Buenos Aires, Buenos Aires, Argentina

⁷University of California, Davis, California 95616

⁸University of California, Irvine, California 92717

⁹University of California, Riverside, California 92521

¹⁰LAFEX, Centro Brasileiro de Pesquisas Físicas, Rio de Janeiro, Brazil

¹¹CINVESTAV, Mexico City, Mexico

¹²Columbia University, New York, New York 10027

¹³Delhi University, Delhi, India 110007

¹⁴Fermi National Accelerator Laboratory, Batavia, Illinois 60510

¹⁵Florida State University, Tallahassee, Florida 32306

¹⁶University of Hawaii, Honolulu, Hawaii 96822

¹⁷University of Illinois at Chicago, Chicago, Illinois 60607

- ¹⁸Indiana University, Bloomington, Indiana 47405
¹⁹Iowa State University, Ames, Iowa 50011
²⁰Korea University, Seoul, Korea
²¹Kyungshung University, Pusan, Korea
²²Lawrence Berkeley National Laboratory and University of California, Berkeley, California 94720
²³University of Maryland, College Park, Maryland 20742
²⁴University of Michigan, Ann Arbor, Michigan 48109
²⁵Michigan State University, East Lansing, Michigan 48824
²⁶Moscow State University, Moscow, Russia
²⁷University of Nebraska, Lincoln, Nebraska 68588
²⁸New York University, New York, New York 10003
²⁹Northeastern University, Boston, Massachusetts 02115
³⁰Northern Illinois University, DeKalb, Illinois 60115
³¹Northwestern University, Evanston, Illinois 60208
³²University of Notre Dame, Notre Dame, Indiana 46556
³³University of Oklahoma, Norman, Oklahoma 73019
³⁴University of Panjab, Chandigarh 16-00-14, India
³⁵Institute for High Energy Physics, 142-284 Protvino, Russia
³⁶Purdue University, West Lafayette, Indiana 47907
³⁷Rice University, Houston, Texas 77251
³⁸Universidade Estadual do Rio de Janeiro, Brazil
³⁹University of Rochester, Rochester, New York 14627
⁴⁰CEA, DAPNIA/Service de Physique des Particules, CE-SACLAY, France
⁴¹Seoul National University, Seoul, Korea
⁴²State University of New York, Stony Brook, New York 11794
⁴³Tata Institute of Fundamental Research, Colaba, Bombay 400005, India
⁴⁴University of Texas, Arlington, Texas 76019
⁴⁵Texas A&M University, College Station, Texas 77843

INTRODUCTION

The properties of elastic and diffractive scattering are well-described by the phenomenology of pomeron exchange, where the pomeron is described as a color singlet with quantum numbers of the vacuum (1,2). The landmark paper of Ingelman and Schlein (3) proposed that the observation of jets in diffractive events would probe the partonic nature of the exchanged object (expected to be the pomeron). This paper introduced the field of hard diffractive scattering, which refers to the subset of traditional diffractive interactions that have a high transverse momentum (p_T) scattering.

The study of hard diffractive processes has expanded dramatically in recent years. Results from UA8, HERA, and the TEVATRON include studies of diffractive jet production (4,5), deep inelastic scattering in large rapidity gap events (6), rapidity gaps between high transverse energy jets (7-9), and a search for diffractive W -boson production (5). These results give new insight into the object exchanged in the production of diffractive events. In this note we describe a preliminary search for single diffraction with high transverse momentum jets with the DØ detector at Fermilab for center-of-mass energies $\sqrt{s} = 1800$ GeV and 630 GeV.

HARD SINGLE DIFFRACTION

An experimental signature of hard diffractive events is the presence of a rapidity gap (10,11), (lack of particle production in a rapidity or pseudorapidity² region) along with evidence of a hard scattering (jet production, W production, etc.). Since the pomeron is a color singlet, radiation is suppressed in events with pomeron exchange resulting in large rapidity gaps in these events (12). In hard single diffraction a pomeron is emitted from one of the incident protons and the pomeron undergoes a hard scattering with the second proton, often leaving a rapidity gap in the direction of its parent proton. We examine the process $p + \bar{p} \rightarrow j + j + X$ and look for the presence of a forward rapidity gap along the direction of one of the initial beam particles.

The event generator PYTHIA 5.7 (13) is used to study particle multiplicities for non-diffractive jet events. Generated events are required to have two jets with $E_T > 12$ GeV and $\eta < -1.6$. The multiplicity of particles opposite the jets in the forward region $2 < \eta < 4$ is plotted in Fig. 1(a). The distribution is well described by a negative binomial (NB) fit (smooth curve), with no significant excess of low multiplicity events. That is to say, the expected number of zero multiplicity (background rapidity gap) events is consistent with multiplicity fluctuations in a sample based on the NB distribution. The study may then be repeated for diffractive production using the event generator POMPYT 1.0 (14), which is based on PYTHIA, but allows for the choice of a pomeron as one of the beam particles. The pomeron carries between 1% and 5% of the incident proton momentum, thus in the lab frame the jets produced are typically boosted, and a rapidity gap is expected on the side opposite the jets. Figure 1(b) shows the forward multiplicity distribution from a POMPYT simulation subject to the same kinematic requirements on the jets as the PYTHIA simulation. This sample is clearly dominated by rapidity gap and very low multiplicity events. For this plot a “hard gluon” pomeron structure has been chosen, which is equivalent to a 2-gluon model of the pomeron, a hypothesis which has some experimental support from UA8 (4) and H1 and ZEUS (6).

The existence of a diffractive signal in the experimental data may be observed as a larger number of rapidity gap events in the forward multiplicity distribution than expected from the non-diffractive background. Given sufficient detector resolution, sensitivity, and statistics, two components in the multiplicity distribution may be resolved and the relative fraction of rapidity gap events in excess of expectations from a smoothly falling multiplicity distribution may be estimated.

DATA ANALYSIS

The DØ detector (15) is used to provide experimental information on the fraction of jet events with forward rapidity gaps. This analysis primarily utilizes the uranium-liquid argon calorimeters which have full coverage for a pseudorapidity range of $|\eta| < 4.1$. The transverse segmentation of the projective calorimeter towers is typically $\Delta\eta \times \Delta\phi = 0.1 \times 0.1$. The electromagnetic (EM) section of the calorimeters is used to search for rapidity gaps. The EM section is particularly useful for identifying low energy particles due to its low level of noise and ability to detect neutral pions. A particle is tagged by the deposition of more than 200 MeV of energy in an EM calorimeter tower.

The data used in this study were obtained using an inclusive trigger requiring at least one jet above 15 GeV in E_T or a forward trigger requiring at least two jets above 12 GeV in

²pseudorapidity or $\eta = -\ln[\tan(\frac{\theta}{2})]$, where θ is the polar angle defined relative to the proton beam direction.

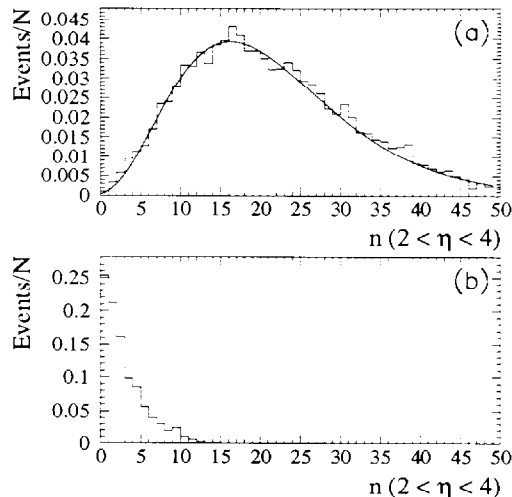


FIG. 1. Particle multiplicities in Monte Carlo Study. (a) Multiplicity of particles produced in the region $2 < \eta < 4$ for PYTHIA events with two jets above 12 GeV in E_T and produced in the region $\eta < -1.6$. (b) Same distribution plotted for a POMPYT (hard diffraction) simulation.

the the region $\eta > 1.6$ or $\eta < -1.6$. As mentioned above, the jet system is expected to be boosted in diffractive jet production, thus a forward trigger can be utilized to provide an enhanced sample of diffractive events. Offline, two jets above trigger threshold are required for events used in the analysis. Events with multiple $p\bar{p}$ interactions are removed from the sample as well as events for which either of the leading two jets fail standard quality cuts (16). Jets are reconstructed using a cone algorithm with radius, $R = \sqrt{\Delta\eta^2 + \Delta\phi^2} = 0.7$. The number of EM towers (n_{EM}) above a 200 MeV energy threshold is measured opposite the leading two jets in the region $2 < |\eta| < 4.1$ for the data. The (n_{EM}) distribution for the forward trigger at 1800 GeV is shown in Fig. 2. This distribution shows a peak at zero multiplicity in qualitative agreement with expectations for a diffractive signal component. The fits shown are a NB fit to the data from $n_{EM} = 3$ to $n_{EM} = 100$ and a fit restricted to the rising edge of the distribution from $n_{EM} = 1$ to $n_{EM} = 14$. Both fits are extrapolated to $n_{EM} = 0$ as a background estimate to the zero multiplicity events. A fractional excess of rapidity gap events is defined to be the number of zero multiplicity events in excess of those predicted by the fit divided by the total number of events in the sample. The fractional excess observed in the forward region is $0.67 \pm 0.05\%$, where the error includes only statistical uncertainties and a systematic error based on the choice of range for the fit. Cross checks indicate that the observed fractional excess is relatively insensitive to the calorimeter energy threshold and that the method of identifying diffractive processes by measuring rapidity gaps is effective in resolving the soft single diffraction component in the total $p\bar{p}$ cross section.

The rapidity gap events are observed to be multiply tagged by other available detectors, including: hadronic calorimeters, forward tracking, beam hodoscopes, and forward muon chambers. However, the effects of various biases on the gap detection efficiency such as noise, multiple $p\bar{p}$ collisions in a single event, particle showering outside of jet cones, and particle production from spectator interactions have not been included in this measurement. Each

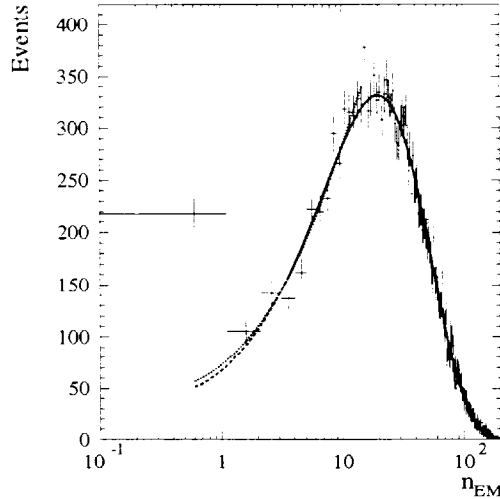


FIG. 2. Number of calorimeter electromagnetic towers (n_{EM}) above a 200 MeV threshold for the region $2 < \eta < 4.1$ opposite the jets in the forward trigger sample. The curves are NB fits to the data excluding low multiplicity bins as described in the text.

of these effects is expected to reduce the number of observed rapidity gaps, thus correcting for these effects is expected to increase the magnitude of the signal measurement.

Multiplicity distributions for the forward trigger data are shown in Fig. 3(a) for both center-of-mass energies. As expected, lower mean multiplicities are produced with decreased center-of-mass energy. An excess of rapidity gap events is also clearly observed at 630 GeV with a magnitude of 1 – 2%. A more complete analysis of systematic effects on the multiplicity measurement must be completed, however, before the two samples can be directly compared.

The boost distribution of the two leading jets for both samples is shown in Fig. 3(b), where the boost is defined as $\eta_{\text{boost}} = (\eta_1 + \eta_2)/2$. The differing boost distributions are consistent with expectations for jet production at the different center-of-mass energies, since less energy is available to produce high E_T objects in the forward regions at lower \sqrt{s} .

The forward gap fraction measurement may be extended to unrestricted jet topologies by use of an inclusive trigger, which provides a sample of events unbiased by any jet pseudorapidity selection. Events are selected with at least two jets of $E_T > 15$ GeV. We divide each trigger sample into subsets based on the measured boost of the leading two jets and plot the forward gap fraction as a function of the average boost in Fig. 4. A clear trend is observed where the forward gap fraction increases with the boost of the jets, although the exact shape may be modified by corrections for the gap detection efficiency.

PRELIMINARY SEARCH FOR HARD DOUBLE POMERON EXCHANGE

The same experimental methods may be applied to a search for hard double pomeron exchange. In this process both incoming protons emit a pomeron and the two pomerons interact to produce a jet system. Rapidity gaps may be produced along each forward beam direction, since there is no color connection between the jet system and the beam

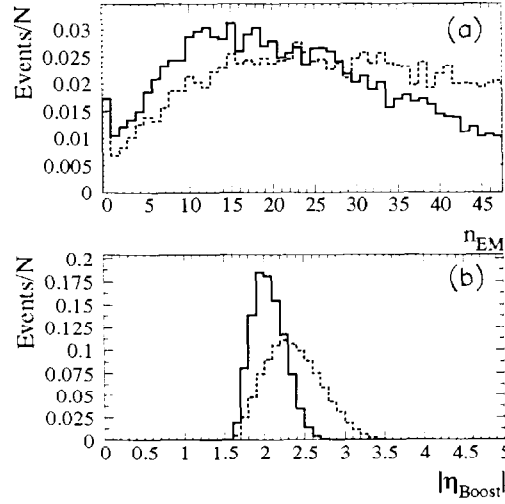


FIG. 3. Comparison of 630 GeV (solid lines) and 1800 GeV (dashed lines) data. (a) Multiplicity distributions of forward electromagnetic towers. (b) Boost distributions for leading two jet system.

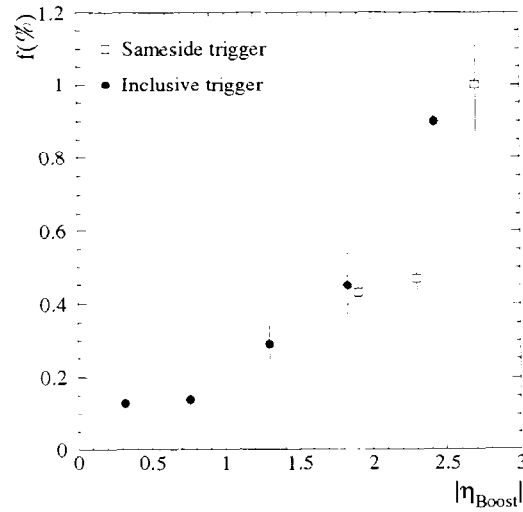


FIG. 4. Forward gap fraction as a function of η_{boost} for the 1800 GeV data. Data from the inclusive trigger are shown in circles, the forward (sameside) trigger data are shown by squares.